European soil NOx emissions derived from satellite NO2 observations

Xiaojuan Lin[1, 2], Ronald van der A[2], Jos de Laat[2], Vincent Huijnen[2], Bas Mijling[2], Jieying Ding[2], Henk Eskes[2], John Douros[2], Mengyao Liu[2], Xin Zhang[3], and Zhu Liu[1]

[1]Department of Earth System Science, Ministry of Education Key Laboratory for Earth System Modeling, Institute for Global Change Studies, Tsinghua University, Beijing, 100084, China.

[2]KNMI, Royal Netherlands Meteorological Institute, De Bilt, 3730 AE, the Netherlands.

[3]SRON Netherlands Institute for Space Research, Leiden, 2333 CA, the Netherlands

Corresponding author: Ronald van der A and Zhu Liu (avander@knmi.nl; zhuliu@tsinghua.edu.cn;)

Key Points:

- An innovative method is introduced to derive soil NO_x emissions in Europe from satellite NO_2 observations.
- The resulting soil NO_x emissions are at least two times larger than widely used bottom-up soil NO_x emission estimates.
- This satellite observation-based method provides a valuable independent estimate of the soil NO_x emissions.

Abstract

We introduce an innovative method to distinguish soil nitrogen oxides (NO_x=NO+NO_2) emissions from satellite-based total NO_x emissions using its seasonal characteristics. To evaluate the approach, we compare the deviation between the tropospheric NO_2 concentration observed by satellite and two atmospheric composition model simulations driven by the newly estimated soil NO_x emissions and the Copernicus Atmosphere Monitoring Service (CAMS) inventory. The estimated average soil NO_x emissions in Europe are 2.5 kg N ha^{-1} yr^{-1} in 2019, and the annual soil NO_x emissions is approximately 2.5 times larger than that of the CAMS inventory. Our method can easily be extended to other regions at middle or high latitudes with similar seasonal characteristics of soil emissions. The soil emissions are subtracted from the total NO_x emissions yielding realistic anthropogenic NO_x emissions. We further show this also yields realistic anthropogenic CO_2 emissions using known CO_2/NO_x factors from bottom-up inventories.

Plain Language Summary

Soil nitrogen oxide emissions (NO_x = NO + NO_2) are an important source of air pollution, accounting for about 15% of global NO_x emissions. Unfortunately, soil emissions are not always accurately described by current bottom-up inventories. Accurate quantification is beneficial for clarifying the contribution of biogenic sources to air quality and developing more targeted air quality measures. We present an innovative method for estimating soil NO_x emissions from satellite-based total NO_x emissions. The newly estimated annual emissions in Europe are about 2.5 times higher than reported in previous studies. The method is evaluated by comparing the deviation between the simulated and satellite observed tropospheric NO_2 concentrations. This method can also be extended to other regions around the world with similar seasonal characteristics of soil NO_x emissions. Anthropogenic NO_x emissions are determined by subtracting the soil NO_x emissions from total NO_x emissions. We further show these anthropogenic NO_x emissions can be converted into realistic CO_2 emissions by using known CO_2/NO_x emission factors.

1 Introduction

Nitrogen oxides (NO_x = NO + NO_2) are important pollutants and their subsequent oxidation products have detrimental impacts on human health and crop production (Skalska et al., 2010). Soil NO_x emissions are the largest contributor to the NO_x budget besides combustion sources, contributing up to ~15% of global NO_x emissions (Hudman *et al.*, 2012; Vinken et al., 2014; Weng et al., 2020). The relative contribution of soil NO_x to total NO_x emissions is gradually increasing due to steadily declining anthropogenic NO_x emissions as a result of successful emission reduction strategies in, e.g., China (van der A et al., 2017; Lu et al., 2021), the USA (Zhang et al., 2003; Silvern et al., 2019), and Europe (Rafaj et al., 2015; Skiba et al., 2020). Furthermore, soil NO_x emissions play a non-negligible role in rural air pollution especially during summer time while fossil fuel combustion emissions are relatively constant over the year (Fortems-Cheiney et al., 2021; Wang et al., 2022). The precise quantification of soil NO_x emissions is therefore essential for assessing emission control strategies and a better understanding of air quality.

Two microbial processes, nitrification and denitrification, are the main sources of soil NO_x and they occur in agricultural and natural ecosystems (Hall et al., 1996; Pilegaard, 2013). Key factors that regulate NO_x emissions from soil are: temperature, soil moisture and texture, soil pH, nutrient availability, ecosystem types, agricultural management and ambient atmospheric NO_x concentration (Hall et al., 1996; Butterbach-Bahl et al., 2013; Medinets et al., 2015). Chamber studies and field measurements are commonly employed to investigate the response of soil NO_x emissions to rewetting of dry soils (Garcia-Montiel et al., 2003; Hickman et al., 2021), fertilizer-induced change (Liu et al., 2017; Song et al., 2020; Hui et al., 2023) and atmospheric deposition (Hall and Matson, 1999; Venterea et al., 2003; Koehler et al., 2009; Eickenscheidt and Brumme, 2012). Global and regional soil NO_x emissions are generally estimated by three different model-based methods: simple scaling (Davidson and Kingerlee, 1997), empirical models (Yienger and Levy II, 1995; Yan et al., 2005; Weng et al., 2020; Simpson and Darras, 2021) and process-oriented models (Butterbach-Bahl et al., 2009; Molina-Herrera et al., 2017). However, these models in general disagree about the soil NO_x quantities and their spatial patterns.

Satellite-based observations provide an alternative method to derive soil NO_x emissions. Bertram et al. (2005) and Zörner et al. (2016) found that SCIAMACHY (Scanning Imaging Absorption spectroMeter for Atmospheric CHartographY) observations captured the brief, high-intensity soil NO_x pulses in response to fertilizer application or rainfall events in agricultural regions and semi-arid ecosystems. Other studies constrained soil NO_x emissions top-down using retrieved NO_2 vertical column densities (VCDs) from the Ozone Monitoring Instrument (OMI) for East China (Lin, 2012) and globally (Vinken et al., 2014) . Huber *et al.* (2020) used the unprecedented spatiotemporal resolution of the TROPOMI NO_2 product to quantify soil-driven contributions of cropland to regional NO_x emissions by a box model on daily to seasonal scales for the U.S. Southern Mississippi River Valley. Furthermore, other studies estimate NO_x emissions by analyzing the relationship between observed NO_2 concentrations and NO_x emissions with inversion techniques that consider the transport process of NO_x (Mijling and van der A, 2012; Miyazaki et al., 2012). However, such methods estimate only total NO_x emissions, encompassing both natural and anthropogenic sources.

In this study, we introduce a new method for estimating soil NO_x emissions in individual grid cells based on its seasonal variations. This method is a post-processing of the total NO_x emissions derived by the inverse algorithm DECSO (Daily Emission estimation Constrained by Satellite Observations, Mijling and van der A, 2012; Ding et al., 2017a) applied to NO_2 observations over Europe by TROPOspheric Monitoring Instrument (TROPOMI) on Sentinel 5 Precursor (S5-P) satellite. We evaluate the performance of our method by comparing the deviation of the tropospheric NO_2 concentrations between atmospheric chemistry model simulations and observations by TROPOMI. Finally, we explore the potential to use the difference between total satellite-derived NO_x emissions and soil NO_x emissions for indirectly estimating fossil-fuel CO_2 emissions.

2 Materials and Methods

2.1 NO_x emissions from DECSO

NO_x emissions are derived by the state-of-the-art inverse algorithm DECSO (Daily Emission estimation Constrained by Satellite Observations, Mijling and van der A, 2012; Ding et al., 2017a). DECSO is specifically developed for daily updates of emissions of short-lived

atmospheric constituents using satellite observations. The algorithm solves the sensitivity of concentrations to emissions using a single forward run of the chemical transport model CHIMERE v2020 (Menut et al., 2021) and a simplified 2D trajectory analysis. An extended Kalman filter is used for assimilation of the observed column concentrations in the inversion step. DECSO is able to provide total emissions from biogenic (originating from soil for NO_x) and anthropogenic sources for short-lived chemical species and it can detect new emission sources that may be missing in bottom-up inventories. It has been validated (Ding et al., 2017b) and successfully applied to different regions using OMI and TROPOMI observations (Ding et al., 2015; Ding et al., 2018; Ding et al., 2020; van der A et al., 2020; Ding et al., 2022). In this study, monthly NO_x emissions in 2019 over Europe (10°W-30°E, 35-55°N) are derived from TROPOMI NO_2 observations using DECSO on a spatial resolution of 0.2° × 0.2°. These total emissions are used as input to isolate soil NO_x emissions in a post-processing step, which is explained below.

2.2 Soil NO_x emissions estimates

Several studies have shown that soil NO_x emissions are significantly influenced by land use type (Valente and Thornton, 1993; Verchot et al., 1999; Yan et al., 2005). The soil emissions in our study area originate from four main land use types: forest, croplands, shrub and grassland (Figure S1). Here we merged shrub and grassland into one category (called "other biogenic") considering their limited occurrence in the study area (Table S1c).

We use the following five steps (see flow chart in Figure S2) to separate soil NO_x emissions from total NO_x emissions:

(1) We select pixels dominated by the biogenic sector using the proportion of each land use type. The minimum thresholds of the three land use ratios (forest, crop, and other biogenic sources) are set to 0.5 for individual grid cells to make sure the cell is dominated by one of the biogenic source sector types. For these pixels, the fraction of urban coverage is required to be less than 0.02 to eliminate the interference of anthropogenic emissions as much as possible. The selected pixels are referred to as biogenic pixels.

(2) To exclude the remaining anthropogenic emissions in the selected grid cells, we subtract CAMS anthropogenic NO_x emissions (version 5.3, called CAMS-ant) from the DECSO total NO_x emissions. Note that this is only done for the selected biogenic pixels. If negative values occur after subtraction, they are set to zero. A sensitivity analysis with respect to this step is described in Section 3.1.

(3) In order to better reflect the spatial heterogeneity of soil emissions, we divide the research area equally into 5 subregions in the latitude direction by 2 subregions in the longitude direction. In each of these 10 subregions, the average monthly emissions of the selected pixels are fitted with a Gaussian function $\boldsymbol{f(x) = A\, e^{\frac{-(x-B)^2}{2C^2}}}$ over one year. We chose a Gaussian function as soil NOx emissions in Europe vary slowly with season with typically a winter minimum and summer maximum. The fitting parameters *A*, *B*, and *C* are obtained for pixels dominated by each of the land use types separately (see step 1). *A* represents the maximum soil NO_x emissions in a year, *B* represents the month when the maximum soil emissions occur, and *C* determines the width of the Gaussian curve and thus the length of the season, which also affects the amount of winter soil NO_x emissions. Examples of the Gaussian fitting can be found in Figure S3.

(4) Since the parameters obtained in step 3 represent soil emissions with a specific land use ratio larger than 0.5 (set in step 1) but still with mixed land use types, we use the solution of formula S2 to obtain the typical parameters of pure pixels, *i.e.* the land use ratio of one of the three types, either forest, crop, or other biogenic sources, equals 1. In this way, we obtain 30 sets of parameters (*A*, *B*, and *C*) representing soil emissions for three land-use types and 10 subregions separately. To smooth the transitions between subregions, we perform a two-dimensional interpolation to obtain the parameters for each land-use type and for each grid cell separately.

(5) We assume that the land use ratio directly determines the proportion of soil NO_x emissions. The monthly soil emissions per grid cell is calculated by multiplying the ratio of the three land use types by the three Gaussian functions of the corresponding soil emission types, and adding them together.

(6) If the soil emission calculated at a certain grid cell is larger than the total emission of DECSO in a certain month, the soil emission of this month is set to be equal to this total emission of DECSO. In this way the total of the derived DECSO emissions remain conserved. The end product will be called DECSO-soil from here.

Figure S4 shows the three key parameters *A*, *B*, and *C* that depict the seasonal characteristics of soil NO_x emissions for the three different land use types, with significant zonal and meridional differentiation. The value of parameter *A*, representing the maximum soil NOx emissions during the year, for forests and croplands are generally similar (Figure S4 a-c). The month of the maximum soil emissions (parameter *B*) occurs a bit later in forest areas (July - August) than in croplands areas (June - July) (see Figure S4 d-f). The parameter *C* represents the width of the Gaussian fit and this also affects winter soil NO_x emissions. For all three land use types, parameter *C* shows a clear decreasing trend with increasing latitude (Figure S4 g-i). This is because the higher the latitude, the lower the winter temperature, and the lower the microbial activity, resulting in a shorter active season.

2.3 Emission inventories and land use dataset

In this study, three emission inventories are used for comparison with our estimates. They are the CAMS soil emissions inventory (CAMS-GLOB-SOIL version 2.4, henceforth called CAMS-soil), the Harvard-NASA Emissions Component (HEMCO) soil emissions inventory (version 2021, called HEMCO-soil) and the National Long-range Transboundary Air Pollution (LRTAP) NO_x emissions (called LRTAP-NO_x). CAMS-soil provides gridded global monthly soil NO emissions as total values and for separate source sectors at spatial resolution of 0.5°×0.5° . It is based on empirical formulas and process parameter models (Simpson and Darras, 2021). HEMCO-soil provides global hourly soil NO_x emissions at a horizontal resolution of 0.25° lat. × 0.3125° lon. (Weng et al., 2020), (Keller et al., 2014). LRTAP-NO_x provide country level yearly NO_x emissions for agriculture and other sectors and is provided by the European Environment Agency. Global monthly bottom-up anthropogenic NO_x (version 5.3, called CAMS-ant) and CO_2 emissions (version 4.2, called CAMS-CO_2) inventories are both obtained from the Copernicus Atmosphere Monitoring Service (CAMS) at a 0.1°×0.1° horizontal resolution (Soulie et al., 2023). All emission data are for 2019 and are regridded to the same domain and resolution of DECSO (0.2° × 0.2°). The land use data Land Cover are obtained from the Copernicus Global Land Service (version3.0.1, Buchhorn et al., 2020). The original 23 land use classes of the Land Cover database were first grouped into 8 new main classes, comprising ocean, urban, cropland,

grassland, bare land, inland water, forest, and shrub defined in Table S1. The land use ratio for each class was calculated by re-gridding the original 100m resolution Land Cover product to the DECSO grid of 0.2°.

2.4 Evaluation of derived soil emissions by comparing modelled concentrations to satellite observations

We conduct two comparative experiments to simulate tropospheric NO_2 columns, which use either CAMS soil emissions or DECSO soil emissions. We evaluate the performance of the newly estimated soil emissions in this study by comparing the Root Mean Square Error (RMSE) between the simulated tropospheric NO_2 concentration and the TROPOMI observed tropospheric NO_2 concentration of these two comparative experiments). The tropospheric NO_2 columns were simulated by an extended version of ECMWF's Integrated Forecasting System (IFS) called "IFS-COMPO" (Flemming et al., 2015; Huijnen et al., 2019). IFS-COMPO is part of the global component of the Copernicus Atmosphere Monitoring Service (CAMS) and has been employed to supply global analyses and forecasts of atmospheric composition in an operational mode starting from 2014. The version of IFS-COMPO employed here is based on IFS CY48R1 (ECMWF, 2023), but with only tropospheric chemistry activated. Its default anthropogenic emissions, based on CAMS-GLOB-ANT v5.3 (Soulie et al., 2023) are adopted. The model is driven by our newly estimated soil NO_x emissions, and CAMS soil NO_x emissions (version 2.4, Simpson and Darras, 2021) for reference. IFS-COMPO was run for the year 2019 at a horizontal resolution of approximately 40 km with 137 vertical layers and 900s time steps and with a one-month spin up period. When we compare TROPOMI NO_2 observations with the IFS-COMPO simulation, only observations with a quality flag above 0.75 are used to avoid retrievals for ground pixels covered with snow, ice or high cloud radiance fraction, as well as problematic retrievals. The model outputs are interpolated to the local overpass time of TROPOMI and the averaging kernel is applied to the modelled NO_2 profile. The collocated observation-model pairs are re-gridded to a regular latitude–longitude grid with a 0.25° resolution using an area-weighted averaging considering the area of the TROPOMI-pixel if the coverage of the grid cell is above 50% (Douros et al., 2023). The only difference between the two comparative model experiments is the input of soil NO_x emissions.

3 Results

3.1 Comparison of Soil NOx emissions with CAMS

Figure 1 shows the spatial distribution of calculated soil NO_x emissions for each sector (forests and croplands sectors) in the study area during summer (May-August). The yearly averaged soil NO_x emissions for the entire domain from forests, croplands, and other biological sources are 2.6, 2.6 and 2.0 kg N ha^{-1} yr^{-1} respectively (in May-August shown in Figure 1 they are on average 3.7, 3.6 and 2.9 kg N ha^{-1} yr^{-1}), which fall within the estimated range of forest emissions (0.35 to 15.9 kg N ha^{-1} yr^{-1} in Saxony of Germany; Molina-Herrera et al. 2017) and are of the same order of magnitude for croplands as estimated by Yan et al. (1.08 kg N ha^{-1} yr^{-1} globally; 2005). Regions with high CAMS-soil emissions, such as the Castile-León plain in Spain and the Po River plain in Italy, display strong similarities with the spatial distribution of DECSO-soil NO_x emissions of the croplands sector (Figure 1 c-d). Furthermore, the CAMS soil NO_x emission inventory has very low emissions in forest areas resulting in lower emission estimates in the northwestern Iberian Peninsula, the forest areas of Romania and the south-central France (Figure 1 a-d). Note

the high correlation (R^2 = 0.53 in Figure S6) between the DECSO forest emissions (Figure 1a) and the difference map shown in Figure 1b.

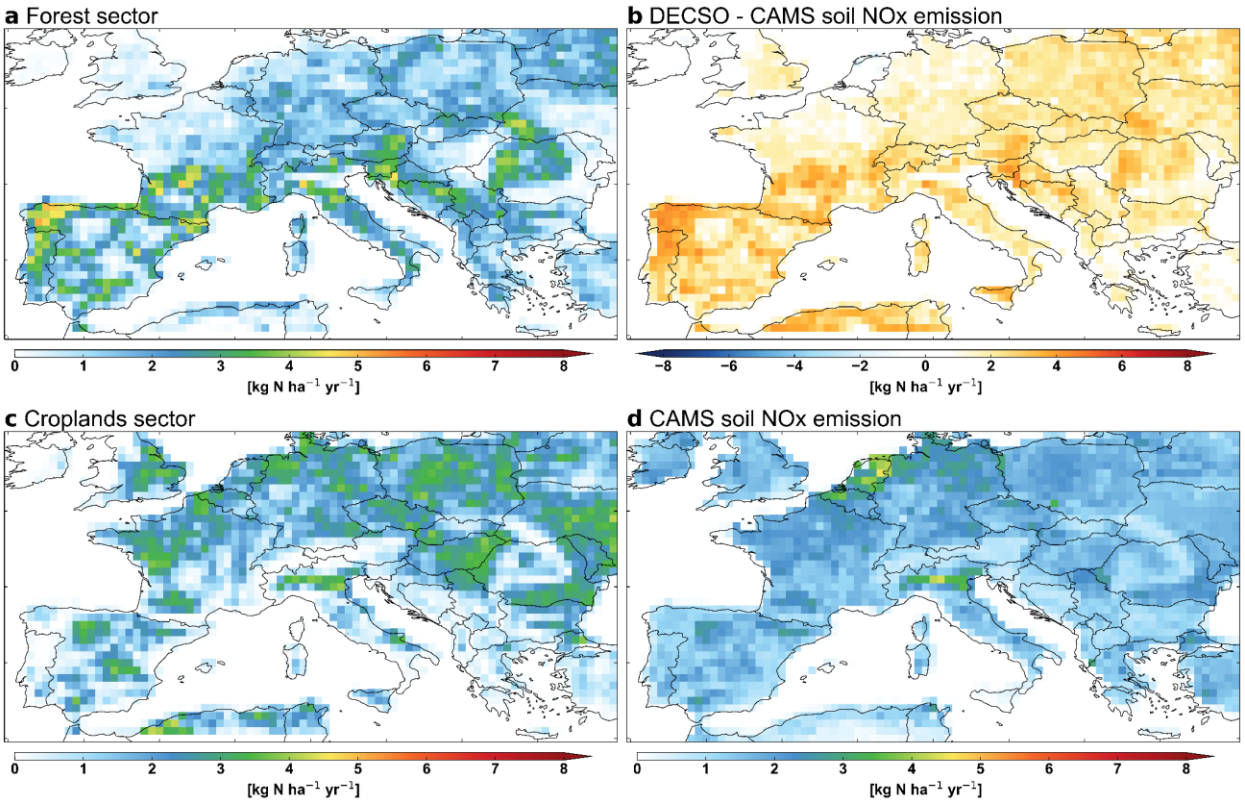

Figure 1. The spatial distribution of the derived soil NO_x emissions during summer represented by the average emissions from May to August in 2019 from (a) forest and (c) croplands. (d) shows the CAMS-soil NO_x emissions in Europe during summer. The difference between CAMS-soil and DECSO-soil is shown in (b). The soil emissions calculated from DECSO total emissions are regridded to the resolution of CAMS-soil, which is 0.5° × 0.5°.

We compared the sum of all DECSO soil to sum of all CAMS soil emissions in our study domain. Our derived total annual soil NO_x emissions are 1.1 Tg N yr^{-1}, which is more than 2.5 times larger than the total of CAMS-soil (0.4 Tg N yr^{-1}) and about 2.3 times higher than HEMCO (0.5 Tg N yr^{-1}) (Figure S7). The average soil NO_x emissions in the study area are 2.5 kg N ha^{-1} yr^{-1} in 2019. Figure 2a shows that the obtained typical monthly time profile of soil NO_x emissions is similar to that of CAMS. The spatial distribution and the amount of the DECSO cropland emissions are comparable to the CAMS soil emissions. CAMS-soil and LRTAP NO_x emissions from agriculture sector are also consistent for national total numbers (Figure 2b). Furthermore, we found that the discrepancy with CAMS is more significant in countries with a large proportion of forest area, such as the Spain (138 Gg N yr^{-1} for DECSO-soil and 48 Gg N yr^{-1} for CAMS-soil) and France (130 Gg N yr^{-1} for DECSO-soil and 64 Gg N yr^{-1} for CAMS-soil). And the deviation is smaller in countries with a large proportion of non-forest area (Figure 2b), such as the Netherlands (about 8 Gg N yr^{-1} for both DECSO-soil and CAMS-soil) and Belgium (7 Gg N yr^{-1} for DECSO-soil and 5 Gg N yr^{-1} for CAMS-soil). Figures 2c and S8 show that after excluding soil emissions, the difference between anthropogenic NO_x emissions derived with DECSO based on satellite observations and CAMS anthropogenic emissions becomes noticeably

smaller (DECSO anthropogenic NO_x is 4.9 kg N ha^{-1} yr^{-1} and CAMS-anthropogenic is 4.8 kg N ha^{-1} yr^{-1}).

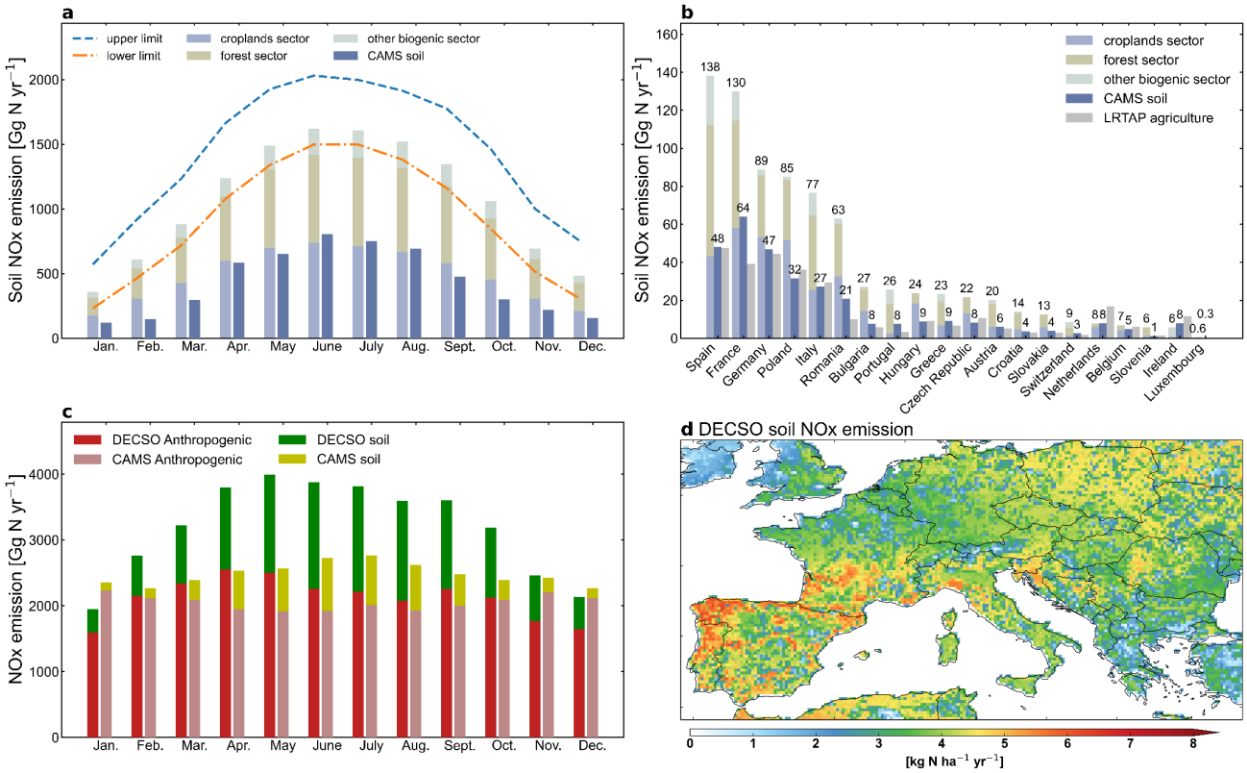

Figure 2. (a) Monthly comparison of derived soil NO_x emissions for three land use types with CAMS-soil. The estimated upper limit and the lower limit of emissions as described in below are shown by the dashed line. (b) National soil NO_x emissions from DECSO-soil and CAMS-soil. (c) The monthly proportion of anthropogenic and soil NOx emissions of DECSO and CAMS. (d) The spatial distributions of DECSO-soil emissions in 2019 during summer (May to August).

3.2 Uncertainty analysis

The biggest uncertainty in our method is caused by the correction for anthropogenic emissions in the selected biogenic grid cells (step 2 in Section 2.2). Therefore, we estimated the upper and lower limit of the calculated soil emissions, by performing a sensitivity test. We first assume all selected biogenic grid cells are without remaining anthropogenic emissions, resulting in an upper limit of the derived soil emissions. On the other hand, the lower limit of emissions is obtained by assuming that the emissions of the selected biogenic grid cells are completely anthropogenic in wintertime as biogenic activity is at a minimum in Europe during winter. Thus we replaced the anthropogenic emissions of CAMS (used in step 2 of Section 2.2) by the average of the DECSO total emissions in January and December. This results in an upper limit of about 33% higher emissions and a lower limit that is about 14% lower than the calculated DECSO-soil emissions (Figure S5).

The derived soil NO_x emissions are sensitive to uncertainties in the derived DECSO emissions. The DECSO emissions have a precision of about 30% for monthly emissions in a single grid cell. However, for this analysis on average soil emissions, the DECSO emissions are averaged over pixels over the whole region and thus strongly reduced compared to single grid cells. Therefore,

the error of the anthropogenic emission correction mentioned above is dominating, and we estimate the uncertainty on the average soil emissions to be about 30%.

3.3 Assessment of the DECSO soil emissions using IFS-COMPO simulations

Figure 3 shows the change of RMSE (ΔRMSE%) between the TROPOMI observations and the simulated tropospheric NO_2 concentration in the IFS-COMPO model driven by the DECSO-soil and CAMS-soil emissions. The smaller the deviation, the higher the reliability of the soil emissions compared to TROPOMI. Figure 3a-d shows the spatial distribution and seasonal variation of ΔRMSE% calculated by formula S3. A negative ΔRMSE% represents that the model simulation deviation driven by DECSO-soil is smaller than that driven by CAMS-soil, meaning that the DECSO-soil are more consistent with TROPOMI observations than that of CAMS-soil. While we use the same TROPOMI NO_2 observations as employed in the DECSO optimization procedure, the atmospheric composition modeling framework is fully independent to DECSO. We found that simulations driven by DECSO soil emissions performed significantly better than using CAMS soil over most of Eastern Europe, North Africa, and Spain (blue area in Figure 3), especially in spring and autumn (Figure S9), when the percentual emissions changes with respect to CAMS-Soil are largest. The spatial distribution of changes in ΔRMSE% in areas dominated by rural area, forest, and croplands area is shown in Figure S10-S12. Overall, the simulated RMSE% of DECSO soil is lower than that of CAMS soil, about 6% lower in spring and 2% lower in autumn (Figure S9). In general, the newly calculated soil emissions significantly reduce the error of the simulated and observed tropospheric NO_2 concentrations, which shows the consistency of the DECSO-soil. The negative ΔRMSE% over forest shows that soil NOx emissions over forest are underestimated by CAMS.

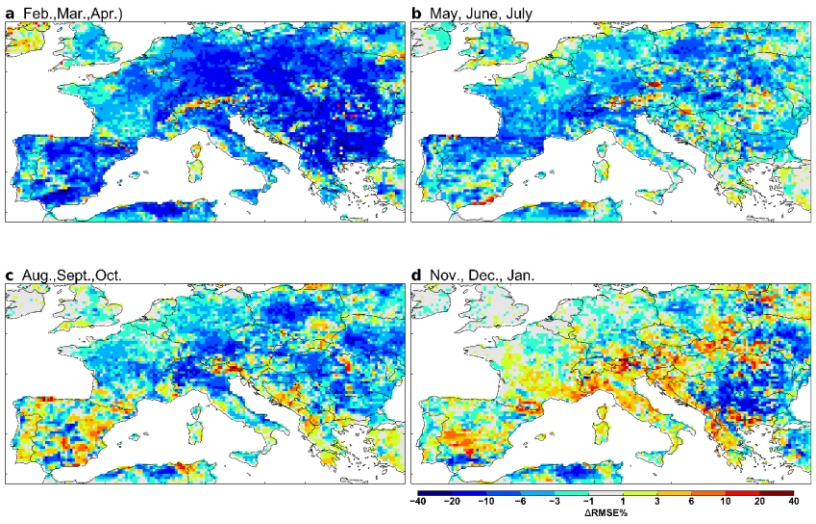

Figure 3. The deviation of observed and simulated tropospheric NO_2 concentrations driven by DECSO-soil and CAMS-soil (a-d) represented by ΔRMSE%. The average of ΔRMSE% in (a) spring, (b) summer, (c) autumn and (d) winter calculated by formula S3. RMSE refers to the average difference between the simulated tropospheric NO2 concentration and the observed tropospheric NO2 concentration. Subtracting RMSE of experiment 2 from that of experiment 1 yields ΔRMSE. Dividing ΔRMSE by the average of the simulated tropospheric NO2 concentration results of the two experiments results in ΔRMSE%. A negative ΔRMSE% shown

in blue means that the DECSO-soil are more consistent with TROPOMI observations than that of CAMS-soil.

3.4 Indirect estimates of anthropogenic CO2 emissions

Since anthropogenic NO_x and CO_2 emissions are usually released simultaneously, several studies have used the NO_x emissions retrieved from satellite observations to infer the anthropogenic CO_2 emissions of countries or regions by a top-down method (de Laat and van der A, 2019; Zheng et al., 2020; Li et al., 2023; Miyazaki and Bowman, 2023). However, these studies did not consider the fact that the NO_x emissions retrieved based on satellite observations include non-anthropogenic soil NO_x emissions. After subtracting soil NO_x emissions from the total NO_x of DECSO, we can calculate the co-emitted CO_2 emissions by multiplying DECSO anthropogenic NO_x emissions with the NO_x/CO_2 emission factors obtained from CAMS inventory. The spatial pattern of CO_2 emissions based on DECSO has a high overall consistency with the bottom-up CAMS emission inventory (Figure 4). The annual CO_2 emissions derived from DECSO (called DECSO-CO2) in the study area in 2019 is 3.7 Gt, which is comparable with the 3.2 Gt of the CAMS inventory (called CAMS-CO2). Overall, this reflects the potential of using DECSO to indirectly infer fossil-fuel CO_2 emissions, especially for regions where CO_2 emissions are less well-known than in Europe.

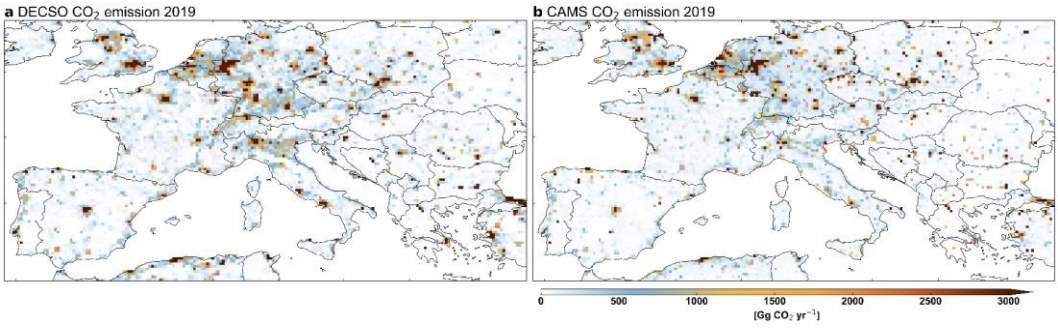

Figure 4. The spatial distributions of (a) estimated annual CO_2 emissions using DECSO, and (b) bottom-up CO_2 emission inventory CAMS.

4 Conclusions

We have developed a method for estimating soil NO_x emissions based on their seasonal characteristics, which we derive from the non-urban regions in our study domain, in our case Europe. The method starts from satellite-based total NOx emissions derived with the DECSO emission inversion system. The estimated soil NO_x emissions based on DECSO is 2.5 kg N ha^{-1} yr^{-1} for Europe in 2019. We found that the existing widely used soil NO_x emission inventories CAMS and HEMCO (based on empirical and statistical models) report lower soil NO_x emissions by about 2.5 times. To assess the reliability of the derived DECSO soil NO_x emissions, we tested them using IFS-COMPO simulations. The model-simulated tropospheric NO_2 concentrations driven by DECSO soil NO_x are closer to the NO_2 concentrations observed by TROPOMI than the simulation driven by CAMS soil emissions. The improvement was especially observed in spring, with a RMSE% reduction of 6%. When checking the spatial distribution (Fig.2), it seems that the discrepancy originates mainly from the forests, where the DECSO derived soil emissions are much higher than those in the CAMS inventory. Possibly the soil NO_x emissions from forests

in Europe are currently underestimated. Not many studies are yet performed to European forest emissions, but Molina-Herrera et al. (2017) concluded that for the state of State of Saxony, Germany both agricultural and forest area are significant sources of soil NO_x .

The seasonal characteristic of DECSO-soil is consistent with the European regional soil NO_x emissions calculated by Simpson and Darras (2021) based on empirical formulas and process parameter models (see Figure S13b). Regions with similar seasonal patterns of soil NO_x emissions as the European region are found at mid-latitudes including North America, North Africa, East Asia, Russia (Figure S13 from Simpson and Darras, 2021) making these regions suitable for deriving soil NOx emissions from satellite with the same approach. For mid-latitude regions in the southern hemisphere such as Australia, this method can also be used by shifting the peak parameter to wintertime.

Our method exploits observations from satellites for a better understanding of the amount and spatiotemporal variation of soil NO_x emissions. The method, starting from DECSO total emissions, is computationally fast and regionally consistent. After isolating the contribution of soil NO_x, the remainder can be attributed to anthropogenic emissions and the total amount and spatial patterns of anthropogenic CO_2 emissions can be indirectly estimated. The results for Europe are consistent with the bottom-up CO_2 inventory, which demonstrate the potential for DECSO to expand its application to other regions in the world with less information on CO_2 emissions.

Acknowledgments

This research has been supported by the project “Sentinel EO-based Emission and Deposition Service” of the European Union's Horizon 2020 research and innovation programme (SEEDS, grant number 101004318). The support provided by the China Scholarship Council (CSC) during a visit by Xiaojuan Lin to the Royal Netherlands Meteorological Institute (KNMI) is acknowledged.

Open Research

TROPOMI data is available at: https://www.tropomi.eu/data-products/nitrogen-dioxide. CAMS soil NOx emissions are available at: https://permalink.aeris-data.fr/CAMS-GLOB-SOIL. HEMCO soil NOx emissions are available at: https://figshare.com/articles/dataset/Global_high-resolution_emissions_of_soil_NOx_sea_salt_aerosols_and_biogenic_VOCs/9962216/4. National Long-range Transboundary Air Pollution (LRTAP) NOx emissions are obtained from the European

Environment Agency (https://www.eea.europa.eu/data-and-maps/dashboards/air-pollutant-emissions-data-viewer-5). CAMS anthropogenic NOx and CO2 emissions are obtained from ECCAD (https://permalink.aeris-data.fr/CAMS-GLOB-ANT). The land use data Land Cover as input data for our method are downloaded from the Copernicus Global Land Service (https://land.copernicus.eu/global/products/lc).

References

Bertram, T. H., Heckel, A., Richter, A., Burrows, J. P. & Cohen, R. C. (2005). Satellite measurements of daily variations in soil NOxemissions. Geophysical Research Letters, 32(24), https://doi.org/10.1029/2005gl024640

Buchhorn, M., Smets, B., Bertels, L., De Roo, B., Lesiv, M., Tsendbazar, N. E., et al. (2020). Copernicus Global Land Service: Land Cover 100m: version 3 Globe 2015-2019: Product User Manual. Zenodo. Geneve, Switzerland.

Butterbach-Bahl, K., Baggs, E. M., Dannenmann, M., Kiese, R. & Zechmeister-Boltenstern, S. (2013). Nitrous oxide emissions from soils: how well do we understand the processes and their controls? Philos Trans R Soc Lond B Biol Sci, 368(1621), 20130122, https://doi.org/10.1098/rstb.2013.0122

Butterbach-Bahl, K., Kahl, M., Mykhayliv, L., Werner, C., Kiese, R. & Li, C. (2009). A European-wide inventory of soil NO emissions using the biogeochemical models DNDC/Forest-DNDC. Atmospheric Environment, 43(7), 1392-1402, https://doi.org/10.1016/j.atmosenv.2008.02.008

Davidson, E. A. & Kingerlee, W. (1997). A global inventory of nitric oxide emissions from soils. Nutrient Cycling in Agroecosystems, 48(1), 37-50, https://doi.org/10.1023/A:1009738715891

de Laat, J. & van der A, R. (2019). CO2 Human Emissions: Fingerprints of fossil CO2 sources. https://www.che-project.eu/sites/default/files/2020-01/CHE-D3-4-V1-0.pdf.

Ding, J., Miyazaki, K., van der A, R. J., Mijling, B., Kurokawa, J.-i., Cho, S., et al. (2017b). Intercomparison of NOx emission inventories over East Asia. Atmospheric Chemistry and Physics, 17(16), 10125-10141, https://doi.org/10.5194/acp-17-10125-2017

Ding, J., van der A, R., Mijling, B., de Laat, J., Eskes, H. & Boersma, K. F. (2022). NOx emissions in India derived from OMI satellite observations. Atmospheric Environment: X, 14(100174, https://doi.org/10.1016/j.aeaoa.2022.100174

Ding, J., van der A, R. J., Eskes, H. J., Mijling, B., Stavrakou, T., van Geffen, J. H. G. M. & Veefkind, J. P. (2020). NOx Emissions Reduction and Rebound in China Due to the COVID-19 Crisis. Geophysical Research Letters, 47(19), https://doi.org/10.1029/2020gl089912

Ding, J., van der A, R. J., Mijling, B., Jalkanen, J. P., Johansson, L. & Levelt, P. F. (2018). Maritime NOx Emissions Over Chinese Seas Derived From Satellite Observations. Geophysical Research Letters, 45(4), 2031-2037, https://doi.org/10.1002/2017gl076788

Ding, J., van der A, R. J., Mijling, B. & Levelt, P. F. (2017a). Space-based NOx emission estimates over remote regions improved in DECSO. Atmospheric Measurement Techniques, 10(3), 925-938, https://doi.org/10.5194/amt-10-925-2017

Ding, J., van der A, R. J., Mijling, B., Levelt, P. F. & Hao, N. (2015). NOx emission estimates during the 2014 Youth Olympic Games in Nanjing. Atmospheric Chemistry and Physics, 15(16), 9399-9412, https://doi.org/10.5194/acp-15-9399-2015

Douros, J., Eskes, H., van Geffen, J., Boersma, K. F., Compernolle, S., Pinardi, G., et al. (2023). Comparing Sentinel-5P TROPOMI NO2 column observations with the CAMS regional air quality ensemble. Geoscientific Model Development, 16(2), 509-534, https://doi.org/10.5194/gmd-16-509-2023

ECMWF (2023). IFS Documentation CY48R1 - Part VIII: Atmospheric Composition. https://www.ecmwf.int/en/elibrary/81374-ifs-documentation-cy48r1-part-viii-atmospheric-composition.

Eickenscheidt, N. & Brumme, R. (2012). NOx and N2O fluxes in a nitrogen-enriched European spruce forest soil under experimental long-term reduction of nitrogen depositions. Atmospheric Environment, 60(51-58, https://doi.org/https://doi.org/10.1016/j.atmosenv.2012.06.018

Flemming, J., Huijnen, V., Arteta, J., Bechtold, P., Beljaars, A., Blechschmidt, A. M., et al. (2015). Tropospheric chemistry in the Integrated Forecasting System of ECMWF. Geoscientific Model Development, 8(4), 975-1003, https://doi.org/10.5194/gmd-8-975-2015

Fortems - Cheiney, A., Broquet, G., Pison, I., Saunois, M., Potier, E., Berchet, A., et al. (2021). Analysis of the Anthropogenic and Biogenic NOx Emissions Over 2008–2017: Assessment of the Trends in the 30 Most Populated Urban Areas in Europe. Geophysical Research Letters, 48(11), https://doi.org/10.1029/2020gl092206

Garcia-Montiel, D. C., Steudler, P. A., Piccolo, M., Neill, C., Melillo, J. & Cerri, C. C. (2003). Nitrogen oxide emissions following wetting of dry soils in forest and pastures in Rondônia, Brazil. Biogeochemistry, 64(3), 319-336, https://doi.org/10.1023/A:1024968802018

Hall, S. J. & Matson, P. A. (1999). Nitrogen oxide emissions after nitrogen additions in tropical forests. Nature, 400(6740), 152-155, https://doi.org/10.1038/22094

Hall, S. J., Matson, P. A. & Roth, P. M. (1996). NOx EMISSIONS FROM SOIL: Implications for Air Quality Modeling in Agricultural Regions. Annual Review of Energy and the Environment, 21(1), 311-346, https://doi.org/10.1146/annurev.energy.21.1.311

Hickman, J. E., Kaya, B., Kebede, A., Kandji, S., Fitch, L., Neill, C., et al. (2021). Little Effect of Land Use on N2O and NO Emission Pulses Following Rewetting of Dry Soils Across Seasonally Dry sub - Saharan Africa. Journal of Geophysical Research: Biogeosciences, 126(1), https://doi.org/10.1029/2020jg005742

Huber, D. E., Steiner, A. L. & Kort, E. A. (2020). Daily Cropland Soil NO(x) Emissions Identified by TROPOMI and SMAP. Geophysical Research Letters, 47(22), e2020GL089949, https://doi.org/10.1029/2020GL089949

Hudman, R. C., Moore, N. E., Mebust, A. K., Martin, R. V., Russell, A. R., Valin, L. C. & Cohen, R. C. (2012). Steps towards a mechanistic model of global soil nitric oxide emissions: implementation and space based-constraints. Atmospheric Chemistry and Physics, 12(16), 7779-7795, https://doi.org/10.5194/acp-12-7779-2012

Hui, K., Yuan, Y., Xi, B. & Tan, W. (2023). A review of the factors affecting the emission of the ozone chemical precursors VOCs and NO(x) from the soil. Environment International, 172(107799, https://doi.org/10.1016/j.envint.2023.107799

Huijnen, V., Pozzer, A., Arteta, J., Brasseur, G., Bouarar, I., Chabrillat, S., et al. (2019). Quantifying uncertainties due to chemistry modelling – evaluation of tropospheric composition simulations in the CAMS model (cycle 43R1). Geoscientific Model Development, 12(4), 1725-1752, https://doi.org/10.5194/gmd-12-1725-2019

Keller, C. A., Long, M. S., Yantosca, R. M., Da Silva, A. M., Pawson, S. & Jacob, D. J. (2014). HEMCO v1.0: a versatile, ESMF-compliant component for calculating emissions in atmospheric models. Geoscientific Model Development, 7(4), 1409-1417, https://doi.org/10.5194/gmd-7-1409-2014

Koehler, B., Corre, M. D., Veldkamp, E., Wullaert, H. & Wright, S. J. (2009). Immediate and long-term nitrogen oxide emissions from tropical forest soils exposed to elevated nitrogen input. Global Change Biology, 15(8), 2049-2066, https://doi.org/https://doi.org/10.1111/j.1365-2486.2008.01826.x

Li, H., Zheng, B., Ciais, P., Boersma, K. F., Riess, T. C. V. W., Martin, R. V., et al. (2023). Satellite reveals a steep decline in China's CO2 emissions in early 2022. Science Advances, 9(29), eadg7429, https://doi.org/doi:10.1126/sciadv.adg7429

Lin, J. T. (2012). Satellite constraint for emissions of nitrogen oxides from anthropogenic, lightning and soil sources over East China on a high-resolution grid. Atmospheric Chemistry and Physics, 12(6), 2881-2898, https://doi.org/10.5194/acp-12-2881-2012

Liu, S., Lin, F., Wu, S., Ji, C., Sun, Y., Jin, Y., et al. (2017). A meta-analysis of fertilizer-induced soil NO and combined NO+N(2) O emissions. Glob Chang Biol, 23(6), 2520-2532, https://doi.org/10.1111/gcb.13485

Lu, X., Ye, X., Zhou, M., Zhao, Y., Weng, H., Kong, H., et al. (2021). The underappreciated role of agricultural soil nitrogen oxide emissions in ozone pollution regulation in North China. Nat Commun, 12(1), 5021, https://doi.org/10.1038/s41467-021-25147-9

Medinets, S., Skiba, U., Rennenberg, H. & Butterbach-Bahl, K. (2015). A review of soil NO transformation: Associated processes and possible physiological significance on organisms. Soil Biology and Biochemistry, 80(92-117, https://doi.org/10.1016/j.soilbio.2014.09.025

Menut, L., Bessagnet, B., Briant, R., Cholakian, A., Couvidat, F., Mailler, S., et al. (2021). The CHIMERE v2020r1 online chemistry-transport model. Geoscientific Model Development, 14(11), 6781-6811, https://doi.org/10.5194/gmd-14-6781-2021

Mijling, B. & van der A, R. J. (2012). Using daily satellite observations to estimate emissions of short-lived air pollutants on a mesoscopic scale. Journal of Geophysical Research-Atmospheres, 117(20, https://doi.org/10.1029/2012jd017817

Miyazaki, K. & Bowman, K. (2023). Predictability of fossil fuel CO2 from air quality emissions. Nat Commun, 14(1), 1604, https://doi.org/10.1038/s41467-023-37264-8

Miyazaki, K., Eskes, H. J. & Sudo, K. (2012). Global NOx emission estimates derived from an assimilation of OMI tropospheric NO2 columns. Atmospheric Chemistry and Physics, 12(5), 2263-2288, https://doi.org/10.5194/acp-12-2263-2012

Molina-Herrera, S., Haas, E., Grote, R., Kiese, R., Klatt, S., Kraus, D., et al. (2017). Importance of soil NO emissions for the total atmospheric NOx budget of Saxony, Germany. Atmospheric Environment, 152(61-76, https://doi.org/10.1016/j.atmosenv.2016.12.022

Pilegaard, K. (2013). Processes regulating nitric oxide emissions from soils. Philosophical Transactions of the Royal Society B: Biological Sciences, 368(1621), 20130126, https://doi.org/doi:10.1098/rstb.2013.0126

Rafaj, P., Amann, M., Siri, J. & Wuester, H. (2015). Changes in European greenhouse gas and air pollutant emissions 1960–2010: decomposition of determining factors. Uncertainties in Greenhouse Gas Inventories: Expanding Our Perspective, 27-54,

Silvern, R. F., Jacob, D. J., Mickley, L. J., Sulprizio, M. P., Travis, K. R., Marais, E. A., et al. (2019). Using satellite observations of tropospheric NO2 columns to infer long-term trends in US NOx emissions: the importance of accounting for the free tropospheric NO2 background. Atmospheric Chemistry and Physics, 19(13), 8863-8878, https://doi.org/10.5194/acp-19-8863-2019

Simpson, D. & Darras, S. (2021). Global soil NO emissions for Atmospheric Chemical Transport Modelling: CAMS-GLOB-SOIL v2.2. Earth System Science Data Discussions, 2021(1-35, https://doi.org/10.5194/essd-2021-221

Skalska, K., Miller, J. S. & Ledakowicz, S. (2010). Trends in NO(x) abatement: a review. Sci Total Environ, 408(19), 3976-3989, https://doi.org/10.1016/j.scitotenv.2010.06.001

Skiba, U., Medinets, S., Cardenas, L. M., Carnell, E. J., Hutchings, N. & Amon, B. (2020). Assessing the contribution of soil NOx emissions to European atmospheric pollution. Environmental Research Letters, https://doi.org/10.1088/1748-9326/abd2f2

Song, L., Drewer, J., Zhu, B., Zhou, M., Cowan, N., Levy, P. & Skiba, U. (2020). The impact of atmospheric N deposition and N fertilizer type on soil nitric oxide and nitrous oxide fluxes from agricultural and forest Eutric Regosols. Biology and Fertility of Soils, 56(7), 1077-1090, https://doi.org/10.1007/s00374-020-01485-6

Soulie, A., Granier, C., Darras, S., Zilbermann, N., Doumbia, T., Guevara, M., et al. (2023). Global Anthropogenic Emissions (CAMS-GLOB-ANT) for the Copernicus Atmosphere Monitoring Service Simulations of Air Quality Forecasts and Reanalyses. Earth System Science Data Discussions, 2023(1-45, https://doi.org/10.5194/essd-2023-306

Valente, R. J. & Thornton, F. C. (1993). Emissions of NO from soil at a rural site in central Tennessee. Journal of Geophysical Research: Atmospheres, 98(D9), 16745-16753, https://doi.org/https://doi.org/10.1029/93JD01417

van der A, R. J., de Laat, A. T. J., Ding, J. & Eskes, H. J. (2020). Connecting the dots: NOx emissions along a West Siberian natural gas pipeline. npj Climate and Atmospheric Science, 3(1), https://doi.org/10.1038/s41612-020-0119-z

van der A, R. J., Mijling, B., Ding, J., Koukouli, M. E., Liu, F., Li, Q., et al. (2017). Cleaning up the air: effectiveness of air quality policy for SO2 and NOx emissions in China. Atmospheric Chemistry and Physics, 17(3), 1775-1789, https://doi.org/10.5194/acp-17-1775-2017

Venterea, R. T., Groffman, P. M., Verchot, L. V., Magill, A. H., Aber, J. D. & Steudler, P. A. (2003). Nitrogen oxide gas emissions from temperate forest soils receiving long-term nitrogen inputs. Global Change Biology, 9(3), 346-357, https://doi.org/https://doi.org/10.1046/j.1365-2486.2003.00591.x

Verchot, L. V., Davidson, E. A., Cattânio, H., Ackerman, I. L., Erickson, H. E. & Keller, M. (1999). Land use change and biogeochemical controls of nitrogen oxide emissions from soils in eastern Amazonia. Global Biogeochemical Cycles, 13(1), 31-46, https://doi.org/https://doi.org/10.1029/1998GB900019

Vinken, G. C. M., Boersma, K. F., Maasakkers, J. D., Adon, M. & Martin, R. V. (2014). Worldwide biogenic soil NOx emissions inferred from OMI NO2 observations. Atmospheric Chemistry and Physics, 14(18), 10363-10381, https://doi.org/10.5194/acp-14-10363-2014

Wang, R., Bei, N., Wu, J., Li, X., Liu, S., Yu, J., et al. (2022). Cropland nitrogen dioxide emissions and effects on the ozone pollution in the North China plain. Environmental Pollution, 294(118617, https://doi.org/https://doi.org/10.1016/j.envpol.2021.118617

Weng, H., Lin, J., Martin, R., Millet, D. B., Jaegle, L., Ridley, D., et al. (2020). Global high-resolution emissions of soil NOx, sea salt aerosols, and biogenic volatile organic compounds. Sci Data, 7(1), 148, https://doi.org/10.1038/s41597-020-0488-5

Yan, X., Ohara, T. & Akimoto, H. (2005). Statistical modeling of global soil NOxemissions. Global Biogeochemical Cycles, 19(3), https://doi.org/10.1029/2004gb002276

Yienger, J. J. & Levy II, H. (1995). Empirical model of global soil-biogenic NOχ emissions. Journal of Geophysical Research: Atmospheres, 100(D6), 11447-11464, https://doi.org/https://doi.org/10.1029/95JD00370

Zhang, R., Tie, X. & Bond, D. W. (2003). Impacts of anthropogenic and natural NOx sources over the U.S. on tropospheric chemistry. Proceedings of the National Academy of Sciences, 100(4), 1505-1509, https://doi.org/doi:10.1073/pnas.252763799

Zheng, B., Geng, G. N., Ciais, P., Davis, S. J., Martin, R. V., Meng, J., et al. (2020). Satellite-based estimates of decline and rebound in China's CO2 emissions during COVID-19 pandemic. Science Advances, 6(49), https://doi.org/10.1126/sciadv.abd4998

Zörner, J., Penning de Vries, M., Beirle, S., Sihler, H., Veres, P. R., Williams, J. & Wagner, T. (2016). Multi-satellite sensor study on precipitation-induced emission pulses of NOx from soils in semi-arid ecosystems. Atmospheric Chemistry and Physics, 16(14), 9457-9487, https://doi.org/10.5194/acp-16-9457-2016